Journal of Achievements in Materials and Manufacturing Engineering
Volume 63 • Issue 2 • April 2014
International Scientific Journal published monthly by the World Academy of Materials and Manufacturing Engineering

Experimental investigation of damping properties of unidirectionally and fabric reinforced plastics by the free decay method

M. Romano [a], M. Micklitz, F. Olbrich [b], R. Bierl [b], I. Ehrlich [a,*], N. Gebbeken [c]

[a] Laboratory of Composite Technology (LFT), Department of Mechanical Engineering, Ostbayerische Technische Hochschule Regensburg, Galgenbergstrasse 30, 93053 Regensburg, Germany

[b] Sensorik-ApplikationsZentrum (SappZ), Department of General Science and Microsystems Engineering, Ostbayerische Technische Hochschule Regensburg, Seybothstrasse 2, 93053 Regensburg, Germany

[c] Department of Civil Engineering and Environmental Sciences, Institute of Engineering Mechanics and Structural Analysis, University of the Bundeswehr Munich, Werner-Heisenberg-Weg 39, 85577 Neubiberg, Germany

* Corresponding e-mail address: ingo.ehrlich@oth-regensburg.de

Received 18.01.2014; published in revised form 01.04.2014

ABSTRACT

Purpose: of this paper is experimental investigation of damping properties of unidirectionally and fabric reinforced plastics by the free decay method.

Design/methodology/approach: For the evaluation of the presumed effect experimental structural dynamic investigations comparing unidirectionally and fabric reinforced plastics are carried out. In detail the free decay behaviour of flat beamlike specimens under fixed-free boundary conditions and relatively constant and reproducible displacement excitation is investigated.

Findings: The vibrating structure has been measured by a laser scanning vibrometer PSV 400 from POLYTEC. In both cases evaluation of the results yields enhanced damping properties of the specimens with fabric reinforcement compared to the unidirectionally reinforced specimens. The results justify the presumed acting of a mesomechanic kinematic.

Research limitations/implications: The results show that in either case the material damping in terms of the logarithmic decrement of the fabric reinforced material is higher than the material damping in of the unidirectionally reinforced material. Additionally, when the fabric reinforced specimens are addressed, in each case the plain weave reinforced specimens exhibited higher values of the material damping as the twill weave 2/2 reinforced ones.

Originality/value: Ondulations in fabrics as a textile semi-finished product are caused by the alternating crossing of warp and fill yarns. In the mesoscopic scale the acting of a mesomechanic kinematic is presumed to enhance the damping properties under cyclic elastic deformation. For the evaluation of the presumed effect experimental structural dynamic investigations comparing unidirectionally and fabric reinforced plastics are carried out.

Keywords: Structural vibration; Damping; Fibre reinforced plastics; Mesomechanic scale; Fabric reinforced layer; Ondulation

Reference to this paper should be given in the following way:

M. Romano, M. Micklitz, F. Olbrich, R. Bierl, I. Ehrlich, N. Gebbeken, Experimental investigation of damping properties of unidirectionally and fabric reinforced plastics by the free decay method, Journal of Achievements in Materials and Manufacturing Engineering 63/2 (2014) 65-80.

ANALYSIS AND MODELLING

1. Introduction

Nowadays the use of fibre reinforced plastics become indispensable in many areas in industry. The feature of high stiffness and strength which simultaneously combine low mass allows new design approaches for weight loss, which leads to energy savings, for example in the automotive and aircraft industry. Often damages and especially delaminations due to transversal low-velocity impact damage (so-called barely visible impact damages (BVID)) are reported to influence the dynamic properties of a structure. Yet, not only damages but also a presumed mesomechanic kinematic in fabric reinforced single layers is presumed to influence the structural dynamic properties of fibre reinforced plastics.

Simplified theoretical approaches for fibre reinforced plastics often presume a layup of only unidirectionally reinforced single layers. As a first approach in applied engineering the structural mechanic properties can analytically be determined by the use of so-called micromechanic homogenization theories. These are usually based on the single components' properties, namely matrix and fibre. However, different kinds of fabrics are often applied as reinforcements in the layup of structural parts. In this case homogenization theories reach their limit. The reason therefore is that the mesomechanic geometry of fabric reinforced single layers cannot be considered sufficiently by relatively simple homogenization approaches. Yet, mesomechanic correlations are distinctly different as they significantly influence the mechanical properties of a structure.

2. Research environment

The research environment is the description of the structural dynamic behaviour of unidirectionally and fabric reinforced composites with a polymeric matrix system. Therefore a brief literature review is presented. This leads to several conclusions and to the pursued mechanical principle described thereafter.

2.1. Literature review

Mital, Murthy and Chamis 1996 [13] investigate the micromechanics of plain-weave composites. As a result the effects of the fabric reinforcement have been described analytically and basically verified numerically. The fibre-orientation in the mesoscopic dimension has been described by sinusoid parts in the ondulation region connected by straight parts above and under the ondulated yarn. For means of simplicity and in order to reduce computation time symmetry characteristics has been used in the model. Guan and Gibson 2001 [7] suppose the acting of a mesomechanic mechanism for damping in fabric reinforced composites. Therefore a plain-weave construction is investigated numerically and validated basically by the decay of vibrating flat beam-like specimens. Ballhause 2007 [3] investigates the structural mechanics of dry fabric reinforcements on the mesomechanic level under one- and two-dimensional loading. A failure model is formulated based on the increase of contact forces and simultaneously the reduction of the curvatures in the crossing points between warp and fill yarn under increasing loads. Nakanishi et al. 2007 [14] investigates the damping properties of fabric reinforced composites. Thereby glass fibres as a plain-weave in a polymeric matrix system are considered in numerical investigations. Based on the determined mesomechanic properties flat beam-like specimens have been modelled by means of FE-analyses and investigated up to the third bending mode in vibration. Matsuda et al. 2007 [12] besides the elastic behaviour investigate the viscoplastic parts in plain-weave fabrics. A homogenization theory is developed numerically by considering the in-phase and out-of-phase boundary conditions. Badel, Vidal-Sallé and Boisse 2007 [2] as well as Hivet and Boisse 2008 [8] identify a mesoscopic mechanical behaviour for woven composites. Therefore dry fabrics under biaxial tension are investigated numerically. A strong nonlinearity is reported especially at the beginning of the loading. Ansar, Xinwei and Chouwei 2011 [1] give a review about modelling strategies. Even if 3D woven composites are focused, a parametric consideration of the geometric dimensions is supposed. Correlations between

geometric and technical parameters are indicated, but only treated generally. Additionally different approximations for modelling the cross-section, amongst others a lens-shaped cross-section, of the single tows are listed. Kreikmeier et al. 2011 [11] introduce sine-shaped fibre-orientation in the in-plane direction as an imperfection due to a selected manufacturing process. The sine as an analytical function is processed analytically for a basic description of the phenomenon, yet without parametric variation of the geometric dimensions.

Hivet and Duong 2010 [9] carry out similar numerical investigations for dry fabric reinforcements under shear load conditions. Thereby the load is applied by a picture-frame mechanism. Nonlinearities are detected regarding the angle of deformation and the resulting orientation of the yarns in the fabric. The basic concept and the identification of acting mechanisms have also been investigated basically in Ottawa et al. 2012 [29]. Thereby plain representative sequences of a plain weave fabric have been investigated. The model is investigated using finite element analysis (FEA). The material properties as well as the boundary conditions have parametrically been varied. The elastic response and mesomechanic kinematic due to geometric constraints has further been separated in the evaluation of the results. Additionally a basic validation has been carried out experimentally.

2.2. Presumed mechanical principle

The aim of the carried out experimental investigations is the identification of the influence of a mesomechanic kinematic caused by ondulations in fabric reinforced composites. Therefore the experimental investigations of flat beamlike specimens yield a one-dimensional approach. In the following the simplifying presumptions as well as the mechanical acting principle are briefly described.

Three mechanically different regions can be identified, when a plain representative sequence of a complete ondulation as parametrically shown in Figure 1 left is considered. These are namely warp yarn, weft yarn and surrounding matrix. Regarding their stiffnesses as the characteristic mechanical properties there is:

- the warp yarn with predominant direction following the longitudinal sine and so E_1 following the sine and E_2 perpendicular to it,
- the two fill yarns with predominant direction perpendicular to the cross-section and so $E_2 = E_3$ in the investigated plain model and
- the matrix region that is not reinforced at all with E_{matrix}.

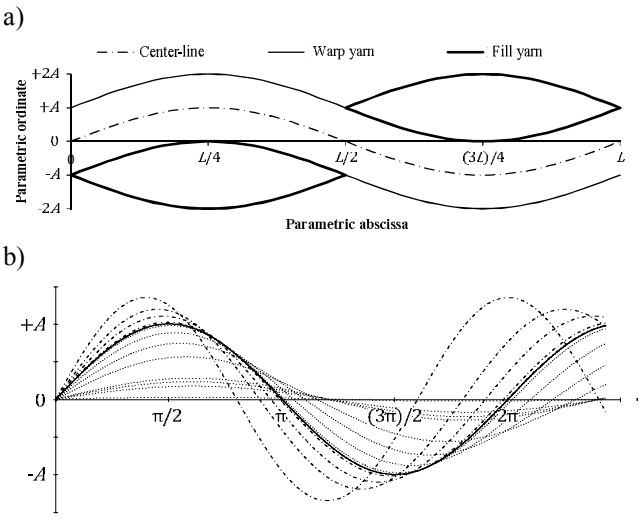

Fig. 1. Plain representative sequence of a fabric reinforced layer based on analytic dimensions A and L of a sine (a). Obtained sine-waves for a sinusoid with A=1 and L=2π: Original graph bold solid line; Elongated graphs as dashed lines; Shortened graphs as dash-dotted lines (b)

There are significant differences in the values of the stiffnesses of the different regions. Thereby the stiffness E_1 of the unidirectionally reinforced yarns is significantly higher in the direction of the reinforcement compared to the stiffness E_2 in direction perpendicular to the reinforcement and the stiffness E_{matrix} of the matrix region. The relations can mathematically be related by

$$E_1 >> E_2 > E_{\text{matrix}} \quad . \tag{1}$$

In case of a unidirectionally reinforced single layer with high tenacity (HT) carbon fibres with a presumed fibre volume content of $\varphi_f = 60\,\%$ common homogenization theories yield $E_1 = 150\text{GPa} >> E_2 = 11.5\,\text{GPa} > E_{\text{matrix}} = 3.3\,\text{GPa}$ in case of carbon fibres as absolute values for the stiffnesses of the different regions. In relative terms it is $E_1 \approx 13 \cdot E_2$ and $E_1 \approx 45 \cdot E_2$, respectively. Under the former described structural mechanical correlations a mesomechanic kinematic can be lead back to geometrical constraints only. Thereby two different effects in the model can be identified, when positively and negatively defined longitudinal deformations are considered. In both cases the unidirectionally reinforced ondulated yarn is subjected to a purely elastic deformation. Additionally at the same time in case of positively defined longitudinal deformations a smoothing or flattening and in case of negatively defined

deformations an upsetting of the unidirectionally reinforced ondulated yarn is induced due to its mesomechanic geometry. In both cases the decrease and the increase of the amplitude is a superposition of transversal contraction due to Poisson effects as a purely elastic response and a purely kinematic response due to geometric constraints in the mesomechanic scale. In contrast longitudinal deformations applied on a unidirectionally reinforced single layer in direction of the reinforcement leads to a lengthening and shortening in longitudinal direction and a transversal contraction directly coupled due to Poisson effects only.

The direct coupling between applied deformation and obtained shift in amplitude due to geometric constraints is illustrated in Figure 1b. Thereby only the centreline of an ondulated yarn is considered. The mesoscopic geometry is idealized by approximating it with an analytical sine curve. For a representative sequence of one complete ondulation

$$y = A \sin\left(2\pi \frac{x}{L}\right) \tag{2}$$

the argument of the trigonometric function is presumed in the interval $(\ldots) \in [0, 2\pi]$ that leads to the domain of definition $x \in [0, L]$. The representative domain of definition can be reduced to the wavelength of one complete ondulation, i.e. $D = [0, L]$ because of symmetry properties [4]. With arbitrary amplitude A and $x \in [0, L]$ the representative domain of the argument in the trigonometric function is obtained. As a strongly simplifying mathematical approach the ondulated yarn is assumed not to lengthen or shorten due to strain or compression but remaining constant in length. Mechanically this presumption can be stated as in term of an infinite high Young's modulus in longitudinal direction and a flexural modulus transverse to it that is presumed to be zero,

$$E_{\mathrm{l}} \to \infty \quad \text{and} \quad E_{\mathrm{b}} \to 0\,, \tag{3}$$

so that an ideally stiff and at the same time ideally flexible yarn is indicated. The sinusoid further is presumed to be fixed at $x = 0$. Positive and negative displacements are applied at the zero-crossing $x = L$. Under the previously stated presumptions a kinematic can be lead back to geometrical constraints only. Figure 1b shows the obtained sine-waves with varying amplitude A and always the same length from its origin at x=0 to its second zero-crossing at $x = L$ for an original sinusoid function. Whereas the bold solid line represent the elongated sequences as dashed lines the shortened sequences are illustrated as dash-dotted lines. For reasons of simplification the amplitude has been set to $A = 1$ and the originally considered argument of the trigonometric function has been presumed to lie in the interval $(\ldots) \in [0, 2\pi]$ due to the domain of definition $x \in [0, L]$.

The repeated acting of this mesomechanic kinematic due to geometric constraints is presumed to enhance the damping properties of fabric reinforced single layers compared to unidirectionally reinforced ones. For an evaluation the free decay behaviour of flat beamlike specimens with fabric reinforced and unidirectionally reinforced single layers are investigated. Thereby the fixed-free boundary condition has been identified as adequate. During the free decay the structure undergoes the kinematic in a number of cycles equal to the fundamental frequency. Thereby the specimens are investigated with selected unsupported lengths so that constant geometric conditions, i.e. with the same unsupported length, and constant dynamic conditions, i.e. with the same fundamental frequency can be evaluated.

3. Materials and test procedures

In the following used materials and production process of the test panels and the preparation of the specimens is described. Additionally the experimental determination of the fibre volume content is explained. The principle of laser vibrometry as a very adequate contactless reference vibrational analysis system is briefly explained. The experimental setup and a detailed description of the carried out structural dynamic investigations is indicated. The respective standards (DIN, EN or ISO) are indicated.

3.1. Materials and processing

Test panels with different kinds of reinforcement, namely unidirectionally reinforced and fabric reinforced, have been produced. For maximum comparability the selection of the materials was done under the requirement that the roving used in the fabric as textile semi-finished product is the same as used for the production of the unidirectionally reinforced single layers. In detail one set of unidirectionally and fabric reinforced prepregs and in case of the dry textile semi-finished products two sets of comparable materials, namely roving, plain weave fabric and twill weave fabric 2/2 have been investigated. For impregnation of the dry textile semi-finished products filament winding according to DIN 65071-1 [16] and pre-impregnation technique according to DIN 65071-2 [17] have been applied.

In case of the prepregs unidirectionally reinforced prepregs Hexcel G947 [20] with a linear density of approx. 200 tex (=3k) and fabric reinforced prepregs Hexcel G939 [20] with an areal weight of approx. 220 g/m² have been used. Both are carbon fibre prepregs with the same warm-curing, thermoset matrix system HexPly M18/1 [20].

In case of the dry textile semi-finished products the first set of comparable materials consists of the roving Tenax HTS40 [27] with a linear density of approx. 800 tex (=12k) provided by Toho Tenax Europe in Wuppertal (Germany), the plain weave fabric is of the kind Style 427 [26] with an areal weight of approx. 400 g/m² and the twill weave fabric 2/2 is of the kind Style 404 [25] with an areal weight of approx. 600 g/m², both provided by ECC in Heek (Germany). The second set of comparable materials consists of the roving Pyrofil TR50S 6K [22] with a linear density of approx. 400 tex (=6k) provided by Grafil Inc. in Sacramento (USA), the plain weave fabric is of the kind Sigratex KDL 8051/120 [24] with an areal weight of approx. 300 g/m² and the twill weave fabric 2/2 is of the kind Sigratex KDL 8052/120 [23] with an areal weight of approx. 300 g/m², both provided by SGL Technologies in Wackersdorf (Germany). Thereby the impregnation of the dry textile semi-finished products was done with the warm-curing, thermoset matrix system Araldite LY 556/Aradur 917/Accelerator DY 070 [15] provided by Huntsman Advanced Materials.

The curing was done by autoclave processing under a vacuum bag. The specimens were cut out of the test panels by waterjet cutting with a nominal lateral dimensions of l_s=250 mm x b=25 mm. The specimens have been measured to determinate the exact geometric dimensions. Whereas length l_s and width b have been measured via calliper, the thickness h has been measured by micrometre. Width b and thickness h have been measured at five equidistantially distributed positions over the length l_s of each specimen. Furthermore the mass m of every specimen was determined by weighting them on a precision balance. Knowing the mass m, the length l_s, the width b and the thickness h the density ρ of the specimen has been calculated by

$$\rho = \frac{m}{V} = \frac{m}{l_s \cdot b \cdot h} \quad . \tag{4}$$

The results for the density ρ have additionally been experimentally determined according to DIN EN ISO 1183-1 [19]. The experimental determination of the fibre volume content is carried out to ensure material quality. In case of organic carbon fibres the fibre volume content is determined by chemical extraction of the fibres according to DIN EN 2564 [18]. Five specimens of every test panel with geometric dimensions of approx. 15 mm x 15 mm have been investigated to ensure a statistical quality. The mass of every specimen was determined by weighing them. The specimens have been placed in concentrated sulphuric acid and have been heated up to 160°C to extract the fibres from the matrix. By adding hydrogen peroxide till the brown coloured solution turns clear again, it is ensured that the fibres have been completely extracted from the matrix. After drying the wet fibres the mass can be determined by weighting them and the fibre volume content φ_f can be calculated.

Knowing the mass of the specimen prior to extracting the fibres m_c and the mass of the remaining fibres m_f the fibre mass content ψ can be calculated by

$$\psi = \frac{m_c}{m_f} , \tag{5}$$

where m indicates the mass and the subscripts f and c indicate the properties of the fibres and of the composite, respectively. The fibre volume content φ_f is then evaluated by

$$\varphi_f = \frac{1}{1 + \frac{1-\psi}{\psi} \cdot \frac{\rho_f}{\rho_m}} , \tag{6}$$

where ρ is the density and ψ is the fibre mass content. The densities of the single components, namely reinforcing fibres and thermoset resin, are taken out of the respective data sheets [15,20, 22-27].

For all test panels and thus the prepared specimens a fibre volume content of approx. $\varphi_f = 55\,\%$ in case of the prepreg material and approx. $\varphi_f = 60\,\%$ in case of the impregnated dry textile semi-finished products has been achieved. Under this presumption the comparability between the single specimens based on one kind of roving can be stated, even though they consist of different kinds of textile types of reinforcement, namely unidirectionally and fabric reinforced single layers. Table 1 resumes the relevant properties of the selected kinds of reinforcements and of the test panels. It demonstrates the former stated comparability of the materials.

3.2. Laser vibrometry as reference vibration analysis system

The vibrating structure is measured by a laser scanning vibrometer of the type PSV 400 from Polytec [21]. For this reason in the following the laser vibrometry and its principle as an adequate reference vibration analysis system is briefly described.

Table 1.
Selected kinds of comparable reinforcements of unidirectionally and fabric reinforced test panels, namely prepregs and dry textile semi-finished products, the corresponding polymeric matrix system and relevant properties of the cured composite

ID	Rein-forcement	Type of material	Linear density/ Areal weight	Matrix system	Kind of fibre reinforcement	Stacking sequence	Density ρ of cured composit	Fibre volume content φ_f	Literature
Ten-Uni	Tenax HTS40	Roving	800 tex (12 k)	Araldite LY 556 Aradur 917/ Acc. DY 070	Unidir. 0° Carbon	$[0]^{C}_{2S}$	1.52	60.0	[15,27]
Ten-Plain	Style 427	Plain weave	400 g/m²	Araldite LY 556 Aradur 917/ Acc. DY 070	Plain weave Warp 0° Carbon	$[(0/90)]^{C}_{2S}$	1.51	61.0	[15,26]
Ten-Twill	Style 404	Twill weave 2/2	600 g/m²	Araldite LY 556 Aradur 917/ Acc. DY 070	Twill weave 2/2 Warp 0° Carbon	$[(0/90)]^{C}_{2S}$	1.52	60.0	[15,25]
Pyr-Uni	Pyrofil TR50S 6K	Roving	400 tex (6 k)	Araldite LY 556 Aradur 917/ Acc. DY 070	Unidir. 0° Carbon	$[0]^{C}_{4S}$	1.54	59.0	[15,22]
Pyr-Plain	Sigratex KDL 8051/120	Plain weave	300 g/m²	Araldite LY 556 Aradur 917/ Acc. DY 070	Plain weave Warp 0° Carbon	$[(0/90)]^{C}_{4S}$	1.53	61.0	[15,24]
Pyr-Twill	Sigratex KDK 8052/120	Twill weave 2/2	300 g/m²	Araldite LY 556 Aradur 917/ Acc. DY 070	Twill weave 2/2 Warp 0° Carbon	$[(0/90)]^{C}_{4S}$	1.54	60.0	[15,23]
Hex-Uni	Hexcel G947 UD	Unidir. prepreg	200 tex (3 k)	HexPly M18/1	Unidir. 0° Carbon	$[0]^{C}_{4S}$	1.52	54.7	[20]
Hex-Fab	Hexcel G939 Fabric	Fabric prepreg	220 g/m²	HexPly M18/1	Plain weave Warp 0° Carbon	$[(0/90)]^{C}_{4S}$	1.51	54.1	[20]

A laser scanning vibrometer enables the experimental measurement of the structural dynamic vibrations of the specimens with the necessary precision and reproducibility. There are no disturbances due to sensors or instrumentations, which would for example represent additional disturbing point masses in the analytical description of the mechanical system. Further laser vibrometry exhibits a high sensitivity and at the same time the capability of measuring a wide range of frequencies. The afore mentioned properties are at the same time the requirements for the carried out experimental investigations. Thus, laser vibrometry enables a relatively simple experimental setup. In detail a laser scanning vibrometer of the type PSV 400 from Polytec [21] has been used. Thereby the velocity of the surface of the vibration structure is measured contactless by a low power laser beam. For further investigations the use of a scanning laser vibrometer offers the additional advantage of being able to rapidly measure a series of test points on the sample surface, when a continuous excitation is used.

In detail laser vibrometry works by targeting a low power laser beam onto a moving surface. The reflected/ scattered light travelling back to the vibrometer receives a Doppler shift of $f_D = 2\frac{v}{\lambda_L}$, where v is the velocity of the surface in the direction of the laser beam source and λ_L is original wave length of the low power laser. Within the device, the reflected laser beam is interfered with a reference laser beam, creating an interference pattern on the detector. Thereby its intensity is varying with time due to the frequency shift of the measurement laser beam and a constant offset frequency shift applied to the reference laser beam through a Bragg cell. The evaluation over the recording time of the measured light intensity yields either the velocity of the surface v when the shift of the frequency is considered or the displacement of the surface w when the shift of phase is considered [10].

3.3. Experimental setup for structural dynamic investigations

For the structural dynamic investigations the specimens are excited to free vibrations by reproducible displacement excitations. Therefore every specimen is defiantly and reproducibly positioned and clamped on one side. Thereby

due to the fixed-free boundary condition the specimens can be treated as cantilever beams. The free decay of the vibrating structure is measured by the laser scanning vibrometer of the type PSV 400 from Polytec [21]. Figure 2a shows the test setup as a schematic side view of the test setup containing from left to right the clamping, the clamped specimen, the side of excitation and the Polytec PSV 400. Figure 2b shows isometric view of the clamping with specimen and excitation.

a)

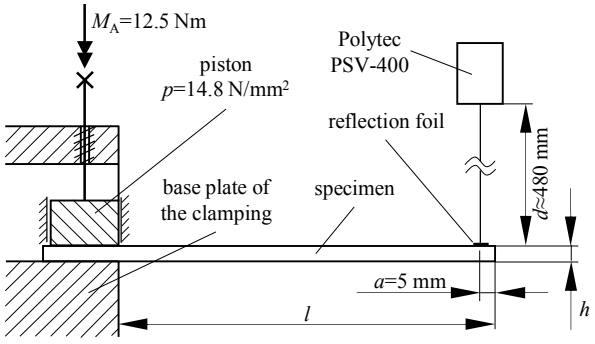

b)

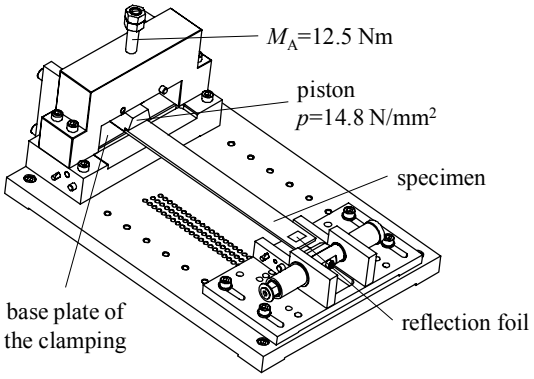

Fig. 2. Schematic side view of the test setup containing from left to right the clamping, the clamped specimen, the side of excitation and the Polytec PSV 400 (a). Isometric view of the clamping with specimen and excitation (b)

In order to reproducibly and definitely excite by displacement the free end is moved by pin. When the value of the amplitude of the free decaying vibration reaches the quarter of the thickness $h/4$ the recording is triggered. In detail a so-called pre-trigger provided by the Polytec software [21] enables this adjustment.

The necessity for this relatively constant displacement for each specimen arises from the requirement to measure the structural dynamic properties in a presumed linear viscoelastic range over the whole recording time of the signal. Non-linear effects that would all have affected especially the measured damping properties must therefore be reduced to a minimum. Geometric non-linearities due to relatively too large displacements as well as non-linearities of the material behaviour or effects of air friction can be neglected by relatively constant displacements. In preliminary investigations the reasonably defined relatively constant displacement of $h/4$ has been identified.

The laser scanning vibrometer measures the velocity of the surface of the vibrating structure over the recording time of the signal. Whereas the shift in frequency of the wave length of the laser enables measuring the velocity of the vibrating surface the shift in phase of the wave length of the laser enables measuring the displacement of the surface of the vibrating structure. Thus the velocity as well as the displacement over the recording time of the signal can further be evaluated. Because for structural mechanics the displacement signal is more reasonable and more descriptive the displacement-time signal has been processed and evaluated further.

In the software of signal processor of the laser scanning vibrometer PSV 400 from Polytec [21] the settings for recording the signals are defined in terms of the bandwidth B and the number of lines in the frequency domain N [21]. The selected bandwidth is B=1000 Hz. The number of lines in the frequency domain is set to N=12800. These settings yield the sampling rate $f_s = 2.56 \cdot B = 2560$ Hz and the total recording time of $t_{tot} = N/B$ =12.8 s for each single measurement of the free decay behaviour. The corresponding resolution in the frequency domain is $f_r = 1/t_{tot} = B/N$ =78.125 mHz [21].

In detail three specimens for each kind of reinforcement are measured. In order to achieve statistically ensured results every specimen has been measured five times in a row. This requirement allows calculating an average value with a respective standard deviation for each specimen and each kind of reinforcement.

4. Results and discussion

In the following the evaluation of the experimental results in terms of displacement over recording time of the signal is described in the time domain as well as in the frequency domain. The structural dynamic investigations of the specimens under the presumption of constant geometric conditions and under constant dynamic conditions are explained. Finally the results are discussed.

4.1. Evaluation of experimental results

The unidirectionally reinforced specimens are considered as the basis of the experimental investigations because no acting of the presumed mesomechanic kinematic is assumed. In case of the dry textile semi-finished products the basic unsupported length of the unidirectionally reinforced specimens is l=220 mm due to the nominally greater stiffness and respective higher fundamental frequency f in contrast to the fabric reinforced specimens. In case of the prepregs the basic unsupported length of the unidirectionally reinforced specimens is l=200 mm because they exhibit a little smaller thickness h and thus a distinctly smaller geometric moment of inertia I that yield nearly the same natural frequency f for the fabric reinforced specimens

In order to achieve constant geometric conditions the fabric reinforced specimens are investigated with the same unsupported length l=220 mm. Under the same geometric conditions the results of the fabric reinforced specimens with an unsupported length l=220 mm yield lower fundamental frequencies f because of the lower stiffness of the material. With the given unsupported length l and the evaluated fundamental frequency f the overall elastic modulus E of the material of the specimen is calculated by [5,6,28,30]

$$E = \left(\frac{2\pi}{\lambda^2} f\, l^2\right)^2 \frac{\rho A}{I} = 12\left(\frac{2\pi}{\lambda^2} f\, l^2\right)^2 \frac{\rho}{h^2}\ , \tag{7}$$

where l is the unsupported length, f is the fundamental frequency, I is the geometric moment of inertia, ρ the density, A is the area of the cross-section and h is the thickness of the specimen. For the given fixed-free boundary conditions on the edges and the resulting vibrating cantilever beam the wave number of the first eigenvalue λ is determined by the general solution of the homogeneous differential equation of the shear stiff beam according to Euler-Bernoulli. It yields the wave number λ=1.875 for the fundamental frequency as the fundamental frequency of the beam as a structural element [5,6,28,30].

In order to achieve comparable constant dynamic conditions additional structural dynamic investigations with varied unsupported length l of the fabric reinforced specimens have been carried out. Therefore the unsupported length l of the fabric reinforced specimens is varied so that the specimens yield the same fundamental frequency as the unidirectionally reinforced specimens with an unsupported length of l=220 mm. Thereby the dynamic conditions can be considered as being identic and thus comparable. The relation is obtained by solving equation (7) for the unsupported length [5,6,28,30]

$$l = \sqrt{\frac{\lambda^2}{2\pi f}\cdot\sqrt{\frac{EI}{\rho A}}} = \sqrt{\frac{\lambda^2 h}{2\pi f}\cdot\sqrt{\frac{E}{12\rho}}} \tag{8}$$

where f is set to the fundamental frequency of the unidirectionally reinforced specimens with an unsupported length of l=220 mm in case of the two sets of comparable specimens based on the dry textile semi-finished products and l=200 mm in case of the set of comparable specimens based on preprags.

As a verification for measuring and considering only the presumed linear viscoelastic range and avoiding geometric and physical non-linearities the recording time of the signal is divided in five isochronous intervals

$$I(n) = \left[\frac{t_{\text{tot}}}{5}\cdot(n-1), \frac{t_{\text{tot}}}{5}\cdot(n)\right] \quad \text{for} \quad n = 1, \ldots, 5\ , \tag{9}$$

where t is the time, n is the counter for the interval and the subscript *tot* indicates the total recording time of the signal. With the afore mentioned recording time of t_{tot}=12.8 s each isochronous time interval is t_{n}=2.56 s for n=1, …, 5.

Each displacement-time signal for the whole recording time of the signal is transformed into the frequency domain by applying the algorithm of the Fast Fourier Transform (FFT). In contrast the displacement-time signal for each resulting sub-signal $I(n)$ for n=1, …, 5 is considered in the time domain. Evaluation of the signals in the frequency domain yields the fundamental frequency f and thus the dynamic moduli in terms of storage and loss modulus. Evaluation of the sub-signals in the time domain yields the damping properties of each specimen in terms of the logarithmic decrement [5,6,28,30]

$$\Lambda = \frac{1}{n}\cdot\ln\frac{w(t_i)}{w(t_{i+n})} \quad \text{for } n = 1, 2, \ldots, n\ , \tag{10}$$

where n is the counter for the maximum amplitudes in the displacement-time signal and t_i and t_{i+n} is the instant of time of their appearance. For the sub-signals in each case the first and the last maximum amplitude has been used for the evaluation of the logarithmic decrement Λ.

Based on the experimental structural dynamic investigations the so-called dynamic or complex modulus

$$E^* = E' + i\,E'' = (1 + i\,\eta)E'\,, \tag{11}$$

is evaluated with the recorded signal in the time domain. A detailed derivation of the processing is given in Gibson 2000 [5] and Gibson 2012 [6], in the guideline VDI 3830 [28] as well as in Schmidt 2003 [30]. Thereby E' is the storage modulus, E'' is the loss modulus and $\eta = \frac{1}{2\pi}\frac{\Delta W}{W}$ is the loss factor. The latter represents the relation between

the energy dissipated in one complete load cycle and the maximal total energy stored in the structure. Under the presumption of weak damping $D^2 << 1$, where D is the dimensionless Lehr damping factor, the Eigen angular frequency of the damped system ω_d is approximately the Eigen angular frequency of the undamped system ω_0, because $\omega_d = \omega_0 \sqrt{1-D^2}$. That is why the overall elastic modulus E of the material of the specimen according to equation (7) is approximately the storage modulus [5,6,28,30]

$$E' \approx E \quad , \tag{12}$$

representing the real part of the dynamic modulus E^*. It can directly be calculated by evaluating the recorded signal in the time domain. The loss modulus E'', representing the complex part of the dynamic modulus E^*, is approximately calculated by assuming the correlations of a damped harmonic oscillator. Therefore the logarithmic decrement Λ according to equation (10) is evaluated for the recorded signal in the time domain. The correlation $D = \frac{\Lambda}{\sqrt{4\pi^2+\Lambda^2}} \approx \frac{\Lambda}{2\pi}$ yields the dimensionless Lehr damping factor in term of the logarithmic decrement Λ for presumed weak damping of the structure. Additionally the decay constant δ can be expressed in term of the dimensionless Lehr damping factor by $\delta = D\,\omega_0$. The correlation between loss modulus E'' and storage modulus E' can finally be expressed as a correlation in term of the decay constant δ and the Eigen angular frequency of the undamped system ω_0 by [5,6,28,30]

$$\frac{E''}{E'} = \frac{2\,\delta\,\omega_d}{\omega_0^2} \approx \frac{2\,\delta}{\omega_0} \quad . \tag{13}$$

The correlation stated in equation (13) as an approximation for presumed weak damping can be solved for the loss modulus E'' in terms of the logarithmic decrement Λ as previously described and yields [5,6,28,30]

$$E'' = \frac{2\,\delta}{\omega_0} E' = \frac{2\,D\,\omega_0}{\omega_0} E' = 2\,D\,E' = 2\frac{\Lambda}{\sqrt{4\pi^2+\Lambda^2}} E' \approx \frac{\Lambda}{\pi} E' \quad . \tag{14}$$

Thereby the logarithmic decrement Λ is directly evaluated according to equation (10) based on the recorded signal in the time domain and the exact term instead of the approximating term is evaluated for the results.

In detail the afore described evaluation of the results is carried out in MATLAB.

4.2. Results

In the following the results under the presumption of constant geometric conditions and under constant dynamic conditions are illustrated graphically and briefly described.

Figure 3 graphically illustrates the logarithmic decrement Λ for the investigated specimens in the isochronous intervals $I(n)$ for n=1, …, 5 in terms of the average value and the standard deviation. Whereas the upper row of Figure 3 shows the results of the first set of comparable specimens based on the roving Tenax HTS40 [27] (cf. Table 1 IDs Ten-Uni, Ten-Plain and Ten-Twill), the mid row shows the results of the second set of comparable specimens based on the roving Pyrofil TR50S 6K [22] (cf. Table 1 IDs Pyr-Uni, Pyr-Plain and Pyr-Twill) and the lower row shows the results of the Hexcel prepreg material G947 and G939 [20] (cf. Table 1 IDs Hex-Uni and Hex-Fab). Thereby the left column of Figure 3 illustrates the results based on the presumption of constant geometric conditions and the right column of Figure 3 illustrates the results based on the presumption of constant dynamic conditions.

Figure 4 illustrates the storage modulus E' and loss modulus E'' as real and imaginary part of the dynamic modulus E^* for every specimen in the isochronous intervals $I(n)$ for n=1, …, 5 in terms of the average value and the standard deviation. On the left of Figure 4 the results obtained under the presumption of constant geometric conditions and on the right the results obtained under the presumption of constant dynamic conditions are illustrated.

Table 2 resumes the evaluated results of the structural dynamic investigations of the single specimens in terms of the logarithmic decrement Λ and the fundamental frequency f as well as in terms of the storage modulus E' and loss modulus E'' as real and imaginary part of the dynamic modulus E^*.

Results based on the presumption of constant geometric conditions and comparable unsupported lengths

The evaluation of the experimental results of the unidirectionally reinforced specimens and the fabric reinforced specimens for the same unsupported length l=220 mm and l=200 mm, respectively, yield the results for the logarithmic decrement Λ for every isochronous interval $I(n)$ for n=1, …, 5. They are graphically illustrated in the left column of Figure 3 in terms of the average value and the standard deviation.

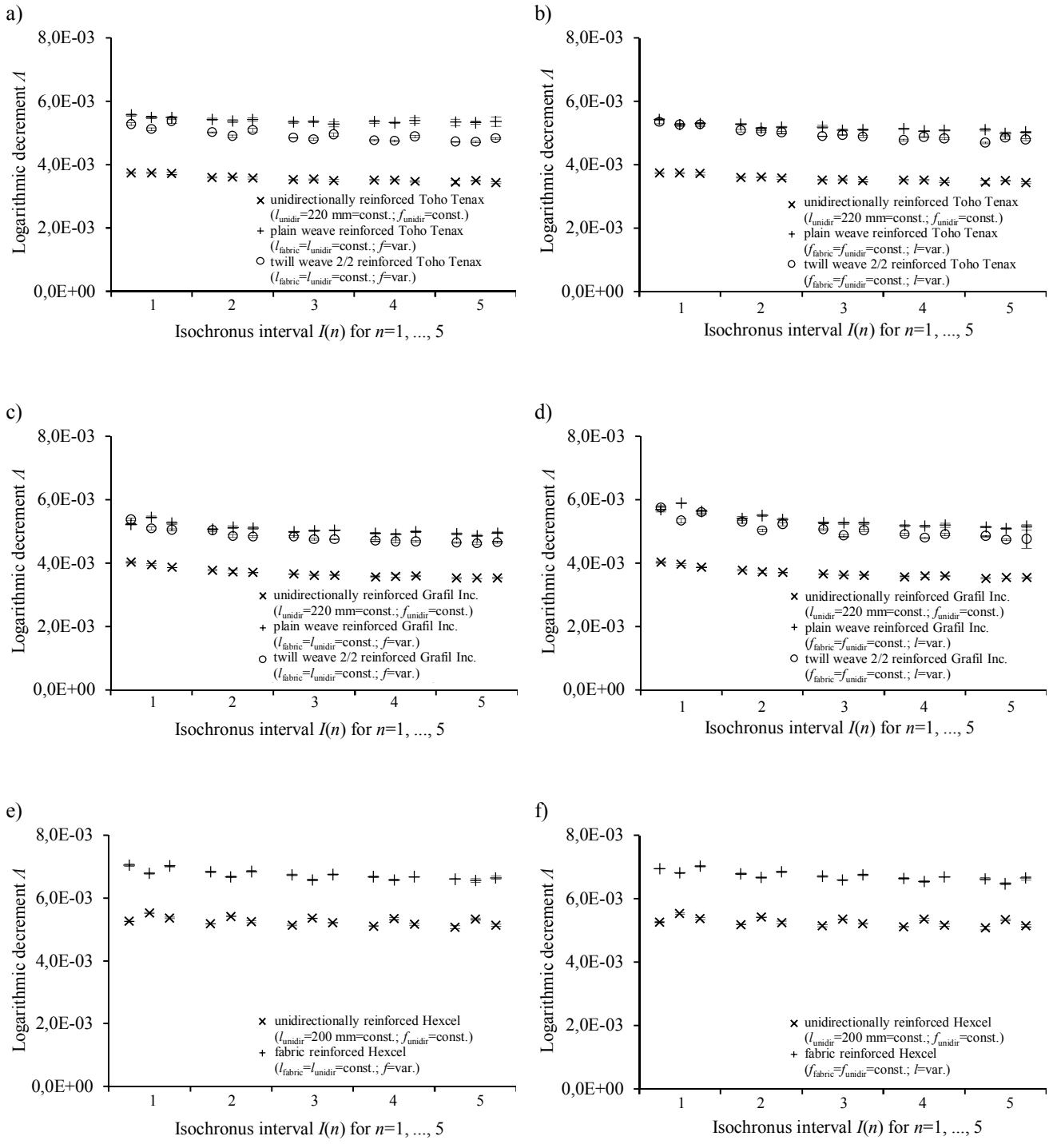

Fig. 3. Logarithmic decrement Λ for every specimen in the isochronous intervals $I(n)$ for n=1, …, 5 in terms of the average value and the standard deviation. a), b): First set of comparable specimens based on the roving Tenax HTS40 [27]. c), d): Second set of comparable specimens based on the roving Pyrofil TR50S 6K [22]. e), f): Hexcel prepreg material G947 and G939 [20]. a), c), e): Under the presumption of constant geometric conditions and comparable unsupported lengths. b), d), f): Under the presumption of constant dynamic conditions and comparable fundamental frequency

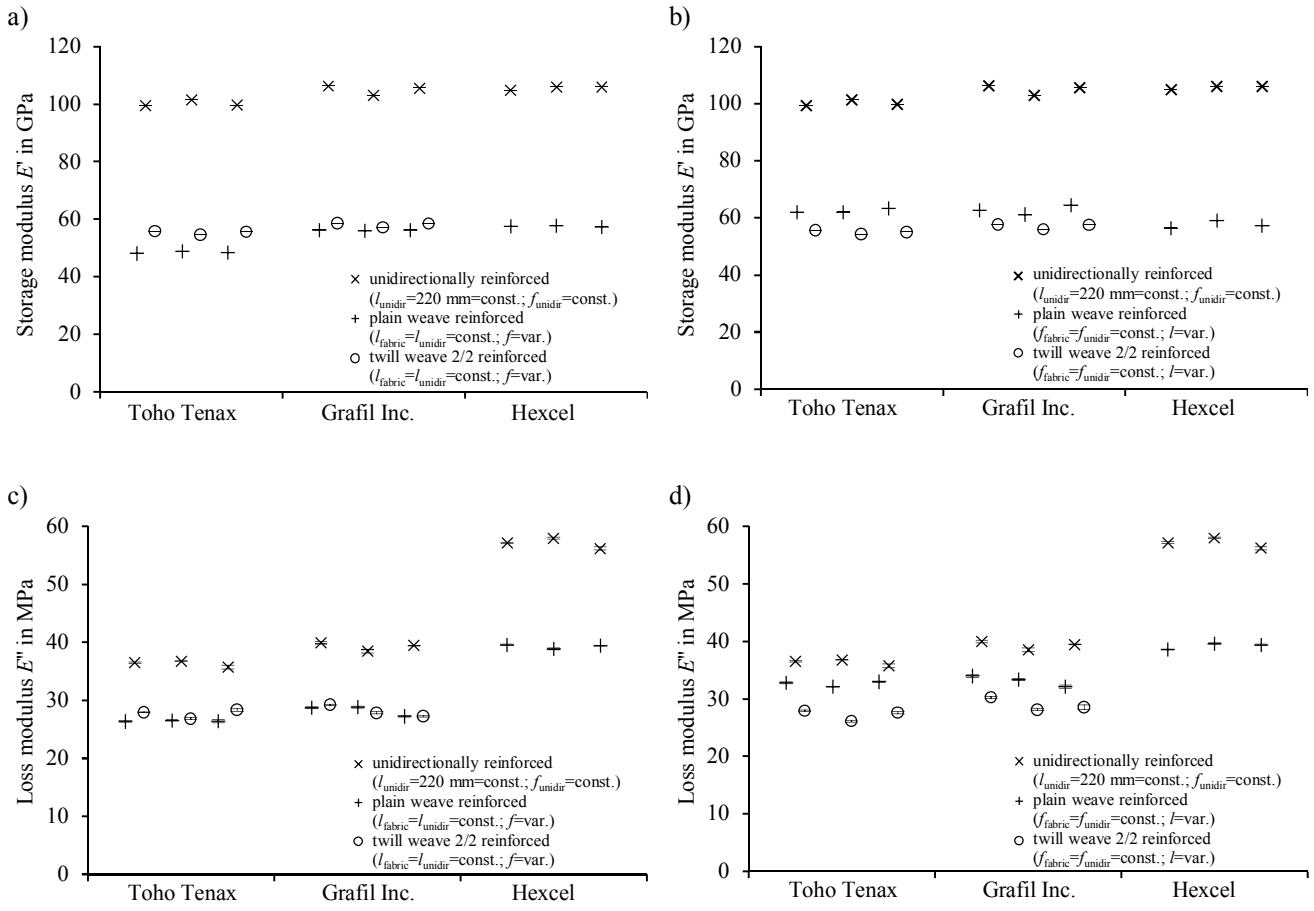

Fig. 4. Storage modulus E' (a, b) and loss modulus E'' (c, d) as real and imaginary part of the dynamic modulus E^* for every specimen in the isochronous intervals $I(n)$ for n=1, …, 5 in terms of the average value and the standard deviation. a), c): Under the presumption of constant geometric conditions and comparable unsupported lengths. b), d): Under the presumption of constant dynamic conditions and comparable fundamental frequency

In case of the first set of comparable specimens based on the roving Tenax HTS40 [27] the average value of the unidirectionally reinforced specimens is Λ=3.56‰. The average value of the corresponding fundamental frequency is f = 50.8 Hz. Regarding the dynamic modulus E* the consideration of the physical and geometrical dimensions yields the storage modulus E' = 100.2 GPa and further consideration of the logarithmic decrement Λ yields the loss modulus E'' = 36.3 MPa . The average value of the plain weave reinforced specimens is Λ=5.39 ‰ with an average value of the corresponding fundamental frequency f=29.9 Hz. In this case the consideration of the physical and geometrical dimensions yields the storage modulus E' = 48.5 GPa and further consideration of the logarithmic decrement Λ yields the loss modulus E'' = 26.5 MPa . The average value of the twill weave 2/2 reinforced specimens is Λ=4.94‰ with an average value of the corresponding fundamental frequency f = 45.42 Hz. In this case the consideration of the physical and geometrical dimensions yields the storage modulus E' = 55.4 GPa and further consideration of the logarithmic decrement Λ yields the loss modulus E'' = 27.7 MPa .

In case of the second set of comparable specimens based on the roving Pyrofil TR50S 6K [22] the average value of the unidirectionally reinforced specimens is Λ=3.96‰. The average value of the corresponding fundamental frequency is f = 55.55 Hz. Regarding the dynamic modulus E* the consideration of the physical and geometrical dimensions yields the storage modulus

$E' = 105.0$ GPa and further consideration of the logarithmic decrement Λ yields the loss modulus $E'' = 39.3$ MPa. The average value of the plain weave reinforced specimens is $\Lambda = 5.06‰$ with an average value of the corresponding fundamental frequency $f = 46.82$ Hz. In this case the consideration of the physical and geometrical dimensions yields the storage modulus $E' = 56.2$ GPa and further consideration of the logarithmic decrement Λ yields the loss modulus $E'' = 28.2$ MPa. The average value of the twill weave 2/2 reinforced specimens is $\Lambda = 4.84‰$ with an average value of the corresponding fundamental frequency $f = 47.37$ Hz. In this case the consideration of the physical and geometrical dimensions yields the storage modulus $E' = 58.1$ GPa and further consideration of the logarithmic decrement Λ yields the loss modulus $E'' = 28.1$ MPa.

Table 2.
Evaluated results of the structural dynamic investigations in terms of the logarithmic decrement Λ and the fundamental frequency f as well as in terms of the storage modulus E' and loss modulus E'' as real and imaginary part of the dynamic modulus E^*

ID	Rein-forcement	Type of material	Stacking sequence	Thickness h (Init. displ. h/4)	Unsupp. length l	Logarithmic decrement Λ	Fundamental frequency f	Storage modulus E'	Loss modulus E''
Ten-Uni	Tenax HTS40	Roving	$[0]^{C}_{2S}$	1.96 mm (0.49 mm)	220 mm	3.56E-03	49.92 Hz	99.44 GPa	36.50 MPa
					220 mm	3.58E-03	51.72 Hz	101.48 GPa	36.78 MPa
					220 mm	3.54E-03	50.63 Hz	99.75 GPa	35.76 MPa
Ten-Plain	Style 427	Plain weave	$[(0/90)]^{C}_{2S}$	1.61 mm (0.40 mm)	220 mm	5.40E-03	29.77 Hz	48.12 GPa	26.35 MPa
					220 mm	5.37E-03	30.16 Hz	48.84 GPa	26.57 MPa
					220 mm	5.39E-03	29.77 Hz	48.40 GPa	26.43 MPa
Ten-Plain	Style 427	Plain weave	$[(0/90)]^{C}_{2S}$	1.61 mm (0.40 mm)	170 mm	5.23E-03	49.69 Hz	61.87 GPa	32.78 MPa
					168 mm	5.11E-03	50.94 Hz	62.05 GPa	32.13 MPa
					168 mm	5.14E-03	51.02 Hz	63.31 GPa	32.96 MPa
Ten-Twill	Style 404	Twill weave 2/2	$[(0/90)]^{C}_{2S}$	2.25 mm (0.56 mm)	220 mm	4.86E-03	45.08 Hz	54.56 GPa	26.85 MPa
					220 mm	4.93E-03	45.63 Hz	55.94 GPa	27.93 MPa
					220 mm	5.03E-03	45.55 Hz	55.70 GPa	28.36 MPa
Ten-Twill	Style 404	Twill weave 2/2	$[(0/90)]^{C}_{2S}$	2.25 mm (0.56 mm)	210 mm	4.99E-03	49.38 Hz	54.35 GPa	26.12 MPa
					206 mm	4.96E-03	51.88 Hz	55.59 GPa	27.93 MPa
					208 mm	4.96E-03	50.63 Hz	54.98 GPa	27.61 MPa
Pyr-Uni	Pyrofil TR 505 6k	Roving	$[0]^{C}_{4S}$	2.07 mm (0.52 mm)	220 mm	3.71E-03	55.47 Hz	106.25 GPa	39.95 MPa
					220 mm	3.69E-03	56.17 Hz	103.03 GPa	38.49 MPa
					220 mm	3.66E-03	55.00 Hz	105.62 GPa	39.48 MPa
Pyr-Plain	Sigratex KDL 8051/120	Plain weave	$[(0/90)]^{C}_{4S}$	2.38 mm (0.60 mm)	220 mm	5.07E-03	46.95 Hz	56.32 GPa	27.22 MPa
					220 mm	5.03E-03	46.88 Hz	56.32 GPa	28.70 MPa
					220 mm	5.08E-03	46.64 Hz	55.99 GPa	28.80 MPa
Pyr-Plain	Sigratex KDL 8051/120	Plain weave	$[(0/90)]^{C}_{4S}$	2.38 mm (0.60 mm)	202 mm	5.32E-03	55.23 Hz	64.44 GPa	32.16 MPa
					200 mm	5.34E-03	56.09 Hz	62.78 GPa	33.96 MPa
					202 mm	5.38E-03	54.92 Hz	61.20 GPa	33.36 MPa
Pyr-Twill	Sigratex KDK 8052/120	Twill weave 2/2	$[(0/90)]^{C}_{4S}$	2.30 mm (0.58 mm)	220 mm	4.92E-03	47.73 Hz	58.61 GPa	29.22 MPa
					220 mm	4.80E-03	47.11 Hz	58.50 GPa	27.25 MPa
					220 mm	4.80E-03	47.27 Hz	57.26 GPa	27.85 MPa
Pyr-Twill	Sigratex KDK 8052/120	Twill weave 2/2	$[(0/90)]^{C}_{4S}$	2.30 mm (0.58 mm)	204 mm	5.18E-03	55.08 Hz	57.69 GPa	30.25 MPa
					202 mm	4.90E-03	55.39 Hz	57.48 GPa	28.57 MPa
					204 mm	5.10E-03	54.38 Hz	56.03 GPa	28.12 MPa
Hex-Uni	Hexcel G947 UD	Unidir. prepreg	$[0]^{C}_{4S}$	1.42 mm (0.34 mm)	200 mm	5.15E-03	42.97 Hz	104.82 GPa	57.14 MPa
					200 mm	5.39E-03	46.80 Hz	106.06 GPa	57.97 MPa
					200 mm	5.23E-03	44.77 Hz	106.07 GPa	56.18 MPa
Hex-Fab	Hexcel G939 Fabric	Fabric prepreg	$[(0/90)]^{C}_{4S}$	1.93 mm (0.48 mm)	200 mm	6.78E-03	44.38 Hz	57.58 GPa	39.58 MPa
					200 mm	6.63E-03	44.53 Hz	57.82 GPa	38.87 MPa
					200 mm	6.79E-03	44.84 Hz	57.29 GPa	39.42 MPa
Hex-Fab	Hexcel G939 Fabric	Fabric prepreg	$[(0/90)]^{C}_{4S}$	1.93 mm (0.48 mm)	204 mm	6.74E-03	42.66 Hz	56.47 GPa	38.55 MPa
					196 mm	6.61E-03	46.41 Hz	59.10 GPa	39.60 MPa
					200 mm	6.79E-03	44.84 Hz	57.29 GPa	39.42 MPa

In case of the Hexcel prepreg material G947 and G939 [20] the average value of the unidirectionally reinforced specimens is $\Lambda = 5.26‰$. The average value of the corresponding fundamental frequency is $f = 44.9$ Hz. for the Hexcel material. Regarding the dynamic modulus E* the consideration of the physical and geometrical dimensions yields the storage modulus $E' = 105.7$ GPa and further consideration of the logarithmic decrement Λ yields the loss modulus $E'' = 57.1$ MPa . The average values of the fabric reinforced specimens is $\Lambda = 6.74‰$ with an average value of the fundamental frequency $f = 44.6$ Hz. In this case the consideration of the physical and geometrical dimensions yields the storage modulus $E' = 57.5$ GPa and further consideration of the logarithmic decrement Λ yields the loss modulus $E'' = 39.3$ MPa .

Results based on the presumption of constant dynamic conditions and comparable fundamental frequency

The evaluation of the experimental results of fabric reinforced specimens under the same dynamic conditions as the unidirectionally reinforced specimens requires varied unsupported lengths l. Therefore the varied unsupported length l required for every plain weave and twill weave 2/2 reinforced specimen has been calculated according to equation (8) based on the results of the original unsupported length. The results of the logarithmic decrement Λ for every isochronous interval $I(n)$ for n=1, …, 5 are evaluated analogue. They are graphically illustrated in the right column of Figure 3 in terms of the average value and the standard deviation where the logarithmic decrement Λ for the fabric reinforced specimens with the varied unsupported lengths l compared to the original results of the unidirectionally reinforced specimens for the original unsupported length. The results represent the same dynamic conditions as comparable fundamental frequencies are addressed.

In case of the first set of comparable specimens based on the roving Tenax HTS40 [27] the average value of the fundamental frequency for the plain weave and twill weave 2/2 reinforced specimens is $f = 50.6$ Hz. Thereby for both kinds of fabric reinforcements it corresponds to the value of the unidirectionally reinforced specimens with original unsupported length $l = 220$ mm. The average value of the plain weave reinforced specimens with varied unsupported length l is Λ=5.16‰. The consideration of the physical and geometrical dimensions yields the storage modulus $E' = 62.4$ GPa and further consideration of the logarithmic decrement Λ yields the loss modulus $E'' = 32.6$ MPa . The average value of the twill weave 2/2 reinforced specimens is $\Lambda = 4.97$ ‰. In this case the consideration of the physical and geometrical dimensions yields the storage modulus $E' = 55.0$ GPa and further consideration of the logarithmic decrement Λ yields the loss modulus $E'' = 27.2$ MPa .

In case of the second set of comparable specimens based on the roving Pyrofil TR50S 6K [22] the average value of the fundamental frequency for the plain weave and twill weave 2/2 reinforced specimens is $f = 55.2$ Hz. Thereby for both kinds of fabric reinforcements it corresponds to the value of the unidirectionally reinforced specimens with original unsupported length $l = 220$ mm. The average value of the plain weave reinforced specimens with varied unsupported length l is $\Lambda = 5.35‰$. The consideration of the physical and geometrical dimensions yields the storage modulus $E' = 62.8$ GPa and further consideration of the logarithmic decrement Λ yields the loss modulus $E'' = 33.2$ MPa . The average value of the twill weave 2/2 reinforced specimens is $\Lambda = 5.08‰$. In this case the consideration of the physical and geometrical dimensions yields the storage modulus $E' = 57.1$ GPa and further consideration of the logarithmic decrement Λ yields the loss modulus $E'' = 29.0$ MPa .

In case of the Hexcel prepreg material G947 and G939 [20] the average value of the fabric reinforced specimens with varied unsupported length l is $\Lambda = 6.71‰$. The average value of the corresponding fundamental frequency is $f = 44.9$ Hz. In this case it corresponds to the value of the unidirectionally reinforced specimens with original unsupported length $l = 200$ mm. The consideration of the physical and geometrical dimensions yields the storage modulus $E' = 57.6$ GPa and further consideration of the logarithmic decrement Λ yields the loss modulus $E'' = 39.2$ MPa .

5. Conclusions and outlook

Specimens with generally different kinds of fibre reinforcement, namely unidirectionally and fabric reinforced, have been mechanically characterized by structural dynamic investigations. Thereby the free decay behaviour of flat beamlike specimens has been measured and evaluated by contactless recording the vibrations by a laser scanning vibrometer of the type PSV 400 from Polytec [21]. The evaluation of the recorded signals in both the time domain and the frequency domain allow distinct conclusions considering the structural dynamic properties of the single kinds of reinforcement.

Under both the presumption of constant geometric conditions and under constant dynamic conditions the

relatively low standard deviations are an indicator for a high degree of reproducibility of the experimental test procedures as well as for high mechanical quality of the material. Additionally the selected relatively constant displacement for each specimen $h/4$ yields nearly constant values for the logarithmic decrement Λ in the isochronous intervals $I(n)$ for n=1, …, 5 and so over the recording time of t_{tot}=12.8 s. This is a basic verification for measuring linear viscoelastic structural dynamic properties only. Under this conditions it can be assumed, that non-linear effects are avoided in the carried out investigations and further that these can be neglected. The indicated non-linearities could be geometric ones due to relatively too large displacements as well as caused by the material behaviour or effects of air friction. The identified relatively constant displacement of $h/4$ can thereby be stated to be reasonable for further experimental investigations.

Three sets of comparable materials have been investigated. The first and second set consist of unidirectionally reinforced, plain weave and twill weave 2/2 reinforced specimens based on the roving Tenax HTS40 [27] and Pyrofil TR50S 6K [22], respectively. The third set consists of unidirectionally and fabric reinforced Hexcel prepreg material G947 and G939 [20]. In each case the logarithmic decrement Λ of the fabric reinforced specimens is generally higher than the values of the unidirectionally reinforced specimens.

When the results under constant geometric conditions are considered, the damping in terms of the logarithmic decrement Λ of the fabric reinforced specimens is higher as the damping in unidirectionally reinforced specimens. In case of the first set of comparable specimens based on the roving Tenax HTS40 [27] the plain weave and twill weave 2/2 reinforced specimens yield higher damping values of 51.4% and 38.7%, respectively. In case of the second set of comparable specimens based on the roving Pyrofil TR50S 6K [22] the plain weave and twill weave 2/2 reinforced specimens yield higher damping values of 37.2% and 31.3%, respectively. In case of the Hexcel prepreg material G947 and G939 [20] the fabric reinforced specimens yield higher damping values of 28.1%.

An analogue tendency can be observed when the results under constant dynamic conditions are considered. In this case for the three sets of comparable materials the logarithmic decrement Λ of the fabric reinforced specimens with varied unsupported length l is generally higher as the values for the unidirectionally reinforced specimens, too. In case of the first set of comparable specimens based on the roving Tenax HTS40 [27] the plain weave and twill weave 2/2 reinforced specimens yield higher damping values of 45.0% and 39.6%, respectively. In case of the second set of comparable specimens based on the roving Pyrofil TR50S 6K [22] the plain weave and twill weave 2/2 reinforced specimens yield higher damping values of 45.1% and 37.7%, respectively. In case of the Hexcel prepreg material G947 and G939 [20] the fabric reinforced specimens yield higher damping values of 27.7 %.

The storage modulus E' as well as the loss modulus E'' of the plain weave reinforced specimens based on the roving Tenax HTS40 [27] and Pyrofil TR50S 6K [22] exhibit a small dependence upon the fundamental frequency f. Thereby higher fundamental frequencies f yield higher values for the storage modulus E' as well as for the loss modulus E''. In contrast the two parts of the dynamic modulus E^* do not exhibit such a dependence on the fundamental frequency f when the twill weave 2/2 reinforced specimens based on the roving Tenax HTS40 [27] and Pyrofil TR50S 6K [22] or the fabric reinforced Hexcel prepreg material G939 [20] are considered.

The results show that in either case the material damping in terms of the logarithmic decrement of the fabric reinforced material is higher than the material damping in of the unidirectionally reinforced material. Additionally, when the fabric reinforced specimens are addressed, in each case the plain weave reinforced specimens exhibited higher values of the material damping as the twill weave 2/2 reinforced ones.

The described observations justify the initially stated assumption that the repeated acting of the presumed mesomechanic kinematic due to geometric constraints enhances the damping properties of fabric reinforced single layers compared to unidirectionally reinforced ones. The observations further allow the conclusion that the presumed kinematic depends on mesomechanic geometric dimensions. These purely geometric conditions could be indicated in terms of a degree of ondulation, that represents the intensity of the single ondulated yarns in different kinds of fabrics (e.g. plain weave, twill weave, satin etc.).

For an identification of parameters and an analysis of the sensitivity to them further investigations of kinematic correlations due to geometric constraints acting in the mesomechanic scale are necessary. For example numerical investigations using the finite element analysis could focus parametrical variations of geometric dimensions with the aim of identifying a kinematic coupling between longitudinal and transversal deformation. In detail plain representative sequences analogue to Ottawa et al 2012 [29] and briefly introduced in Section 2.2 could parametrically be investigated.

Acknowledgements

The carried out experimental investigations have been enabled by the founded project "Lebensdauerüberwachung von faserverstärkten Kunststoffen auf Basis der strukturdynamischen Werkstoffdämpfung – DAMPSIM", financially supported by the Bayerische Forschungsstiftung (BFS), project no. AZ-1089-13, in cooperation with an industrial partner. In this context it was possible to carry out the experimental investigations with a laser scanning vibrometer of the type PSV 400 from Polytec, Waldbronn.

The authors would like to thank the industrial partner and the found for the excellent collaboration and their financial support. Further thanks go to Mr Bastian Jungbauer, B.Eng. for the production of the test panels and the excellent preparation of the specimens as well as to Ms Carolin Renner for her contribution to the project and Mr Simon Walbrun, B.Eng. for carrying out the evaluation of the recorded signals with MATLAB.

References

[1] M. Ansar, W. Xinwei, Z. Chouwei, Modeling strategies of 3D woven composites – A review. Composite Structures 93 (2011) 1947-1963.

[2] P. Badel, E. Vidal-Sallé, P. Boisse, Computational determination of in-plane shear mechanic behaviour of textile composite reinforcements. Computational Material Science 40 (2007) 439-448.

[3] D. Ballhause, Diskrete Modellierung des Verformungs- und Versagensverhaltens von Gewebemembranen. Dissertation, Universität Stuttgart, Stuttgart, 2007.

[4] I. N. Bronstein, K. A. Semendajew, Taschenbuch der Mathematik. 7. Auflage, Verlag Harri Deutsch, Frankfurt am Main, 2008.

[5] R.F. Gibson, Modal vibration response measurements for characterization of composite materials and structures. Composites Science and Technology 60 (2000) 2769-2780.

[6] R.F. Gibson, Principles of Composite Material Mechanics, 3rd Edition, CRC Press, Boca Raton, 2012.

[7] H. Guan, R.F. Gibson, Micromechanic Models for Damping in Woven Fabric-Reinforced Polymer Matrix Composites, Journal of Composite Materials 35/16 (2001) 1417-1434.

[8] G. Hivet, P. Boisse, Consistent mesoscopic mechanical behavior model for woven composite reinforcements in biaxial tension, Composites Part B: Engineering 39 (2008) 345-361.

[9] G. Hivet, A.V. Duong, A contribution to the analysis of the intrinsic shear behavior of fabrics, Journal of Composite Materials 45/6 (2010) 695-716.

[10] M. Johansmann, G. Siegmund, M. Pineda, Targeting the Limits of Laser Doppler Vibrometry, All Polytec 39 (2005) 1-12.

[11] J. Kreikmeier, D. Chrupalla, I.A. Khattab, D. Krause, Experimentelle und numerische Untersuchungen von CFK mit herstellungsbedingten Fehlstellen, Proceedings of the 10th Magdeburger Maschinenbau-Tage, Magdeburg, 2011.

[12] T. Matsuda, Y. Nimiya, N. Ohno, M. Tokuda, Elastic-viscoplastic behavior of plain-woven GFRP laminates: Homogenization using a reduced domain of anlysis, Composite Structures 79 (2007) 493-500.

[13] S.K. Mital, L.N. Murthy, C.C. Chamis, Simplified Micromechanics of Plain Weave Composites, NASA Technical Memorandum 107165 (1996) 1-12.

[14] Y. Nakanishi, K. Matsumoto, M. Zako, Y. Yamada, Finite element analysis of vibration damping for woven fabric composites, Key Engineering Materials 334-335 (2007) 213-216.

[15] Araldite LY 556/Aradur 917/Accelerator DY 070 - Hot Curing Epoxy Matrix System. Technical data sheet, Huntsman Advanced Materials, 2007.

[16] DIN 65071-1 – Faserverstärkte Formstoffe - Herstellung von Prüfplatten aus unidirektional gewickelten Garnen und Rovings. German standard, Normenstelle Luftfahrt (NL) im DIN Deutsches Institut für Normung e. V., Beuth Verlag, Berlin, 1992.

[17] DIN 65071-2 – Faserverstärkte Formstoffe - Herstellung von Prüfplatten aus flächenförmigen Verstärkungsstoffen. German standard, Normenstelle Luftfahrt (NL) im DIN Deutsches Institut für Normung e. V., Beuth Verlag, Berlin, 1992.

[18] DIN EN 2564 – Luft- und Raumfahrt - Kohlenstoffaser-Laminate - Bestimmung der Faser-, Harz- und Porenanteile. German standard, Normenstelle Luftfahrt (NL) im DIN Deutsches Institut für Normung e.V., Beuth Verlag, Berlin, 1997.

[19] DIN EN ISO 1183-1 – Kunststoffe - Verfahren zur Bestimmung der Dichte von nicht verschäumten Kunststoffen - Teil 1: Eintauchverfahren, Verfahren mit Flüssigkeitspyknometer und Titrationsverfahren. German standard, Normenausschuss Kunststoffe (FNK) im DIN Deutsches Institut für Normung e. V., Beuth Verlag, Berlin, 2010.

[20] HexPly M18/1 - 180 °C curing epoxy matrix - Product Data - Prepreg Properties - HexPly M18/1 G947 UD and G939 Woven Carbon Prepregs. Technical data sheet, Hexcel Corporation, March 2007.

[21] Polytec Scanning Vibrometer PSV 400. Technical handbook, Polytec, Waldbronn, 2013.
[22] Pyrofil TR50S 6K – Typical Fiber Properties. Technical data sheet, Grafil Inc. Sacramento (CA) USA, Sacramento, 2008.
[23] Sigratex KDK 8052/120 – Carbongewebe Köper 2/2 - Technisches Datenblatt. Technical data sheet, SGL Technologies GmbH (Wackersdorf), Wackersdorf, 2012.
[24] Sigratex KDL 8051/120 – Carbongewebe Leinwand - Technisches Datenblatt. Technical data sheet, SGL Technologies GmbH (Wackersdorf), Wackersdorf, 2012.
[25] Style 404 Köpergewebe 2/2 – Technisches Datenblatt. Technical data sheet, ECC Fabrics for Composites, C. Cramer Weberei GmbH & Co. KG, Heek, 2012.
[26] Style 427 Leinwandgewebe - Technisches Datenblatt. Technical data sheet, ECC Fabrics for Composites, C. Cramer Weberei GmbH & Co. KG, Heek, 2012.
[27] Tenax HTS40 - Produktprogramm und Eigenschaften für Tenax HTA/HTS Filamentgarn. Technical data sheet, Toho Tenax Europe GmbH, Wuppertal, 2008.
[28] VDI 3830 - Werkstoff- und Bauteildämpfung - Blatt 1-5. Guideline, VDI-Handbuch Schwingungstechnik, Ausschuss Werkstoff- und Bauteildämpfung im Verein Deutscher Ingenieure (VDI)-Gesellschaft Entwicklung Konstruktion Vertrieb, Düsseldorf, 2004.
[29] P. Ottawa, M. Romano, M. Wagner, I. Ehrlich, N. Gebbeken, The influence of ondulation in fabric reinforced composites on dynamic properties in a mesoscopic scale in composites reinforced with fabrics on the damping behavior, Proceedings of the 11th LS-DYNA Forum, Ulm, 9./10. October, 2012, 171-172.
[30] A. Schmidt, Finite-Elemente-Formulierungen viskoelastischer Werkstoffe mit fraktionalen Zeit-ableitungen. Dissertation, Universität Stuttgart, Stuttgart, 2003.